Chapter 4

Influence of flexoelectricity on the EHD instabilities in nematics : a three-dimensional linear analysis for DC excitation

CHAPTER 4

INFLUENCE OF FLEXOELECTRICITY ON THE EHD INSTABILITIES IN NEMATICS: A THREE-DIMENSIONAL LINEAR ANALYSIS FOR DC EXCITATION

4.1 INTRODUCTION

In this chapter we extend the one-dimensional linear analysis presented in the previous chapter by including the boundary conditions. In addition to confirming the results of the one-dimensional model these calculations predict a new flow pattern of the fluid particles within the convective rolls. We also present some experimental observations in support of the theory.

4.2 THE ELECTROHYDRODYNAMIC EQUATIONS

The geometry considered is the same as that in chapter 3 (Fig.1). When the boundary conditions are taken into account all the variables in the problem become functions of ξ and z. The treatment of the problem presented below follows closely that of Penz and Ford [1] for normal rolls (see chapter 2). The variables appearing in the problem are the two polar angles θ and Φ, the three components of the velocity v_ξ, v_η and v_z, the transverse field E_ξ and the pressure p. We assume solutions of the form

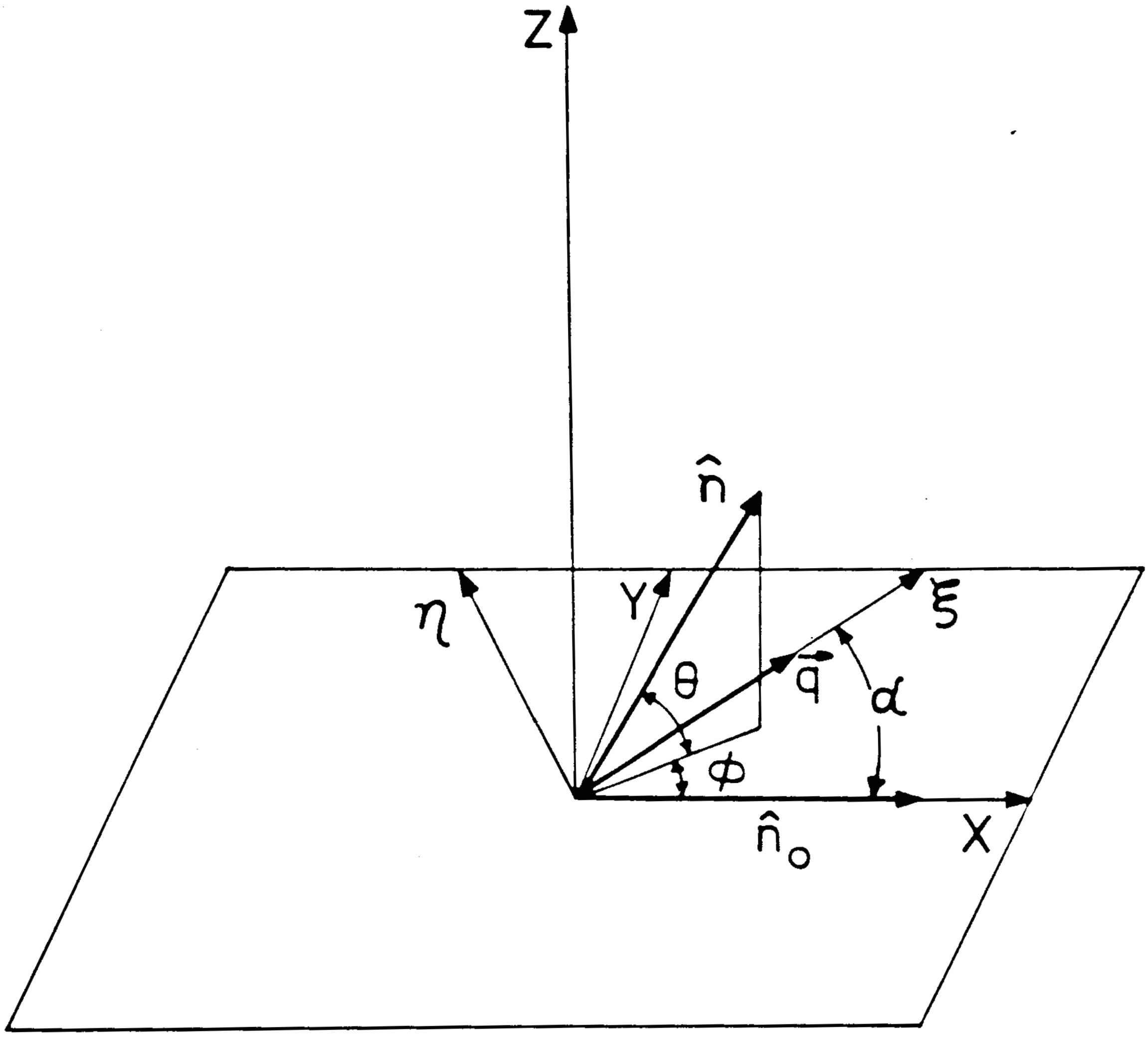

Fig.1. Illustration of the coordinate system and definitions of the angles used in the text.

$$\theta = \theta_o \exp(i\vec{q}.\vec{r}) \ , \ \Phi = \Phi_o \exp(i\vec{q}.\vec{r}),$$
$$E_\xi = E_o \exp(i\vec{q}.\vec{r}) \ , \ v_\xi = - S\, v_o \exp(i\vec{q}.\vec{r}), \qquad (1)$$
$$v_\eta = v_o' \exp(i\vec{q}.\vec{r}) \ , \ v_z = v_o \exp(i\vec{q}.\vec{r}),$$
and $p = p_o \exp(i\vec{q}.\vec{r})$ where $S = q_z / q_\xi$.

The ξ and Z components of the velocity are related by the continuity equation div $\vec{v} = 0$. This leads to a velocity field given by

$$\vec{v} = (-S\, v_z \ , \ v_\eta \ , \ v_z)$$

Since the Maxwell relation curl $\vec{E} = 0$, is to be satisfied, there is a contribution to the Z-component of electric field from the internal field E_ξ. The total electric field is given by

$$\vec{E} = (E_\xi \ , \ 0 \ , \ E_a + S\, E_\xi),$$

where E_a is the applied field. Using the above solutions the following equations describing the system can be set up.

1) The ξ-component of the equation of motion,

$$i\, p_o - [\eta_1 q_z S^2 + \eta_2 q_z]\, v_o - [\eta_3 q_\xi + \eta_4 q_z S\,]\, v_o' = 0 \qquad (2)$$

where $\eta_1 = \frac{1}{2} [a_4 + (a_6 + a_3)\, c^2]$, $\eta_2 = \eta_1 + (a_5 + a_1 c^2)\, c^2$.

$\eta_3 = [a_6 + a_1 c^2]\, s\, c$, $\eta_4 = \frac{1}{2}(a_6 + a_3)\, s\, c$,

$s = \sin a$ and $c = \cos a$.

2) The 7-component of the equation of motion,

$$[2\tilde{\eta}_4 q_\xi q_z + 2\eta_4 q_z^2 S]\, v_o + [\eta_5 q_\xi^2 + \eta_6 q_z^2]\, v_o' = 0 \tag{3}$$

where $\tilde{\eta}_4 = \eta_4 + a_1 c^3 s$, $\eta_5 = a_4 + (a_5 - a_2)c^2 + (a_6 + a_3)s^2 + 2a_1 s^2 c^2$ and $\eta_6 = a_4 + (a_6 + a_3) s^2$.

3) The Z-component of the equation of motion,

$$-iq_z p_o + [\eta_7 q_z^2 + \eta_8 q_\xi^2]v_o + \eta_9 q_\xi q_z v_o' - (e_1 + e_3) E_a q_\xi^2 s c \Phi_o$$
$$+ [\{i\epsilon_a E_a^2 c/4\pi - (e_1 + e_3) E_a q_z c\} q_\xi$$
$$-(iE_a^2/4\pi)(\epsilon_\perp q_z S + \epsilon_c q_\xi)\sigma_1]\theta_o = 0 \tag{4}$$

where $7_7 = \frac{1}{2}[(a_5 + a_2)c^2 - a_4]$, $\eta_8 = \frac{1}{2}[(a_2 - a_5)c^2 - a_4]$,

$\eta_9 = \frac{1}{2}(a_2 + a_5)sc$, $\epsilon_c = \epsilon_\perp + \epsilon_a c^2$, $\sigma_1 = \sigma_a c/[\sigma_\perp(1+S^2) + \sigma_a c^2]$

4) The ξ-component of the torque balance equation,

$$i[(a_2 - a_3 S^4) q_\xi c]v_o - ia_3 q_z s\, v_o' + [R q_\xi q_z - i(e_1 - e_3)E_a q_\xi s]\Phi_o$$
$$+ [M q_\xi^2 + K_1 q_z^2 - i(e_1 + e_3)\sigma_1 E_a^2 q_z c - \epsilon_a E_a^2 \sigma_2/4\pi]\theta_o = 0 \tag{5}$$

where $M = K_2 s^2 + K_3 c^2$, $\sigma_2 = 1 - \sigma_1 c$ and $R = (K_1 - K_2)s$.

5) The Z-component of the torque balance equation,

$$-i\eta_{10} q_z v_o - i\eta_{11} q_\xi v_o' + [R q_z + i\{(e_1 - e_3) - (e_1 + e_3)\sigma_1 c\}E_a s] q_\xi \theta_o$$
$$+ (L q_\xi^2 + K_2 q_z^2)\Phi_o = 0 \tag{6}$$

where $\eta_{10} = (a_2 + a_1)sc$, $\eta_{11} = -a_2 + (a_3 + a_2)s^2$,
and $L = K_1 s^2 + K_3 c^2$.

Eqs.(2-6) form a set of homogeneous equations in the variables θ_o , , v_o , v_o' and p_o . For the existence of non-trivial solutions the determinant of the coefficients of these variables in these equations should vanish. This condition yields the following 12th degree polynomial in S.

$$\sum_{i=0}^{12} a_i S^i = 0 \qquad (7)$$

where S^i is the i^{th} power of S. The coefficients of the polynamial are:

$a_o = M A C_1 - (E_a/q_\xi)^2 [A_1 B_1 C/4\pi + A_2 C_1 + A_3 D_6 s]$,

$a_1 = i(E_a/q_\xi)[AM_{10} - PC_1\sigma_a c - A_3 D_5 s + (E_a/q_\xi)^2 \{-A_1 B_3 c/4\pi + A_2 C_2\}]$,

$a_2 = \sigma_\perp M C_1 - A M_4 - (E_a/q_\xi)^2 [A_1 B_2 c/4\pi - A P B_3 + A_1 B_1 c/4\pi$
$+ (C_1 + C_3)A_2 + A_3 D_2 s + P C_2 \sigma_a c + (e_1 - e_3)\sigma_\perp D_6 s]$,

$a_3 = i(E_a/q_\xi)[A M_9 - D_1 A_3 s - P C_3 \sigma_a c + \sigma_\perp M_{10} - (e_1 - e_3)\sigma_\perp D_5 s$
$+ (E_a/q_\xi)^2 \{(C_2 + C_4)A_2 - A_1 B_3 c/4\pi - A_1 B_5 c/4\pi\}]$,

$a_4 = -A M_3 - \sigma_\perp M_4 - (E_a/q_\xi)^2 [-A P B_5 + A_1 B_4 c/4\pi + A_1 B_2 c/4\pi + A_3 D_4 s$
$+ (C_3 + C_5)A_2 + P C_4 \sigma_a c + (e_1 - e_3)\sigma_\perp D_2 s - \sigma_\perp P B_3]$,

$a_5 = i(E_a/q_\xi)[A M_8 - A_3 D_3 s - P C_5 \sigma_a c + \sigma_\perp M_9 - D_1(e_1 - e_3)\sigma_\perp s$
$+ (E_a/q_\xi)^2 \{C_4 A_2 - A_1 B_5 c/4\pi\}]$,

$a_6 = -A M_2 - \sigma_\perp M_3 - (E_a/q_\xi)^2 [A_1 B_4 c/4\pi + A_1 B_6 c/4\pi + (C_5 + C_6)A_2$
$+ A_3 D_7 s - \sigma_\perp P B_5 + (e_1 - e_3)\sigma_\perp D_4 s]$,

$$a_7 = i(E_a/q_\xi)[(R\ D\ \ -P\ B_6)A - A_3 D_8 s + \sigma_\perp M_8 - (e_1 - e_3)\sigma_\perp D_3 s$$
$$-P\ C_6 \sigma_a c],$$

$$a_8 = -AM_1 - \sigma_\perp M_2 - (E_a/q_\xi)^2 [A_1 B_6 c/4\pi + (C_6 + C_7)A_2 + (e_1 - e_3)\sigma_\perp D_7 s],$$

$$a_9 = i(E_a/q_\xi)[-P\ C_7 \sigma_a c + (R\ D_7 - P\ B_6)\sigma_\perp - (e_1 - e_3)\sigma_\perp D_8 s],$$

$$a_{10} = A\ K_1 C_7 - \sigma_\perp M_1 - (E_a/q_\xi)^2 [A_2 C_7],$$

$$a_{11} = 0,$$

$$a = K_1 \sigma_\perp C_7 .$$

where, $A = \sigma_\perp + \sigma_a c^2$, $A_1 = \epsilon_a \sigma_\perp - \sigma_a \epsilon_\perp$, $A_2 = \epsilon_a \sigma_\perp / 4\pi$,
$A_3 = (e_1 - e_3)A - \sigma_a Pc$, $A_4 = \epsilon_\perp \sigma_a c/4\pi$, $A_5 = A_3 + (e_1 - e_3)A$,
$= A_1 + \epsilon_a A$, $A_8 = \epsilon_a A_3 + (e_1 - e_3)A_1$, $P = (e_1 + e_3)c$, $R = (K_1 - K_2)s$,
$L = K_1 s^a + K_3 c^2$, $M = K_2 s^2 + K_3 c^2$, $N_1 = \eta_5 \eta_{10} - 2\tilde{\eta}_4 \eta_{11}$
$N_2 = 2\tilde{\eta}_4(\eta_3 - \eta_9) + \eta_5(\eta_7 - \eta_2) + \eta_6 \eta_8$,
$N_3 = (\eta_5 a_3 - \eta_6 a_2)c - 2\tilde{\eta}_4 a_3 s$, $N_4 = \eta_6 \eta_{10} - 2\eta_4 \eta_{11}$,
$N_5 = (\eta_6 c - 2\eta_4 s)a_3$, $N_6 = 2\eta_4(\eta_3 + \tilde{\eta}_4 - \eta_9) + \eta_6(\eta_7 - \eta_2) - \eta_1 \eta_5$,
$N = 2\eta_4^2 - \eta_1 \eta_6$, $B_1 = -\eta_5 a_2 L c$, $B_2 = -N_1 R + N_3 L - \eta_5 a_2 K_2 c$,
$B_3 = N_1(e_1 - e_3)s$, $B_4 = -N_4 R + N_3 K_2 + N_5 L$, $B_5 = N_4(e_1 - e_3)s$,
$B_6 = N_5 K_2$ $C_1 = \eta_5 \eta_8 L$, $C_2 = N_1 Ps$, $C_3 = N_2 L + \eta_5 \eta_8 K_2$, $C_4 = N_4 Ps$,
$C_5 = N_2 K_2 + N_6 L$, $C_6 = N_6 K_2 + N_7 L$, $C_7 = N_7 K_2$, $D_1 = N_2 R$, $D_3 = N_6 R$,
$D_2 = (e_1 - e_3)N_2 s + P\ N_3 s$, $D_4 = (e_1 - e_3)N_6 s + P\ N_5 s$, $D_5 = \eta_5 \eta_8 R$,
$D_6 \square \eta_5[\eta_8(e_1 - e_3) - a_2 P\ c]s$, $D_7 = (e_1 - e_3)N_7 s$, $D_8 = NR$,
$M_1 = R\ D_8 - M\ C_7 - K_1 C_6$, $M_2 = R\ D_3 - M\ C_6 - K_1 C_5$,
$M_3 = R\ D_1 - M\ C_5 - K_1 C_3$, $M_4 = R\ D_5 - M\ C_3 - K_1 C_1$,
$M_5 = -[P\ B_1 + M\ C_2 + R\ P\eta_5 a_2 sc]$, $M_6 = -[PB_2 + M\ C_4 + K_1 C_2 - P\ R\ N_3 s]$,
$M = -[P\ B_4 + K_1 C_4 - P\ R\ N_5 s]$, $M_8 = -[P\ B_4 + K_1 C_4 - R\ D_4]$,
$M_9 = -[P\ B_2 + M\ C_4 + K_1 C_2 - R\ D_2]$ and $M_{10} = -[P\ B_1 + M\ C_2 - R\ D_6]$.

Note that all the coefficients of the odd powered terms in the above polynomial are imaginary and proportional to the flexoelectric coefficients. Therefore, when the flexoelectric terms are neglected, all the odd powered terms drop out and Eq.(6) becomes a 6^{th} order polynomial in S^2. Since the coefficients of the even powered terms are all real, the roots of S^2 that are not real occur in complex conjugate pairs. Taking each of these roots with positive and negative signs we get the 12 roots of S.

When the flexoelectric terms are included, the roots of S that are not purely imaginary are complex and occur in pairs of the form (a + ib) and (-a + ib). It may be noted here that roots of this type are also found in the case of the Benard instability in a rotating fluid subjected to a magnetic field [2].

The 12 roots of S can be determined using the 12 boundary conditions that the six variables, viz, θ, Φ, E_ξ, v_ξ, v_η, v_z have to satisfy at the two surfaces. These are:

$$\theta\ (Z = \pm\ d/2) = 0\ ,\ \Phi\ (Z = \pm\ d/2) = 0,$$
$$E_\xi\ (Z = \pm\ d/2) = 0\ ,\ v_4\ (Z = \pm\ d/2) = 0, \qquad (8)$$
$$v_\eta\ (Z = \pm\ d/2) = 0 \text{ and } v_z\ (Z = \pm\ d/2) = 0.$$

Substituting the 12 roots S_j in solutions (1) and using the above conditions, we get 12 equations in S_j and $\delta = q_\xi\, d/2$. For example, the two boundary conditions on v_z lead to the following two equations.

$$\sum_{j=1}^{12} v_j \exp(iS_j\delta) = 0 \tag{9}$$

$$\sum_{j=1}^{12} v_j \exp(-iS_j\delta) = 0 \tag{10}$$

where v_j are arbitrary coefficients. Eqs. (9) and (10) yield, on adding and subtracting, respectively

$$\sum_{j=1}^{12} v_j \cos(S_j\delta) = 0 \tag{11}$$

$$\sum_{j=1}^{12} v_j \sin(S_j\delta) = 0 \tag{12}$$

The other boundary conditions also lead to similar equations. These equations can be written in terms of the coefficients v_j using Eqs.(2-6). Thus we obtain a set of 12 equations in v_j relating the roots S_j and δ. For the existence of solutions satisfying the boundary conditions the 12 x 12 determinant associated with these equations must vanish. This boundary value determinant (BVD) is given by

$$D_{ij} = 0 \qquad ; \; i,j = 1,12 \tag{13}$$

The elements of the determinant are:

$D_{1j} = \cos(S_j \delta)$, $D_{2j} = \sin(S_j \delta)$, $D_{3j} = S_j D_{1j}$,$D_{4j} = S_j D_{2j}$,

$D_{5j} = T_j D_{1j}$, $D_{6j} = T_j D_{2j}$, $D_{7j} = F_j D_{1j}$, $D_{8j} = F_j D_{2j}$, $D_{9j} = G_j D_{1j}$,

$D_{10j} = G_j D_{2j}$, $D_{11j} \square H_j D_{1j}$, $D_{12j} = H_j D_{2j}$.

where,

$T_j = (S_j \tilde{\eta}_4 + S_j^3 \eta_4)/(\eta_5 + S_j^2 \eta_6)$, $F_j = (b_j - c_j)/(d_j - e_j)$,

$G_j = F_j /[\sigma_\perp(1+S_j^2) + \sigma_a \ c^2]$, $H_j = (f_j - g_j)/(d_j - e_j)$, $b_j = m_j n_j$,

$c_j = p_j 1_j$, $d_j = r_j 1_j$, $e_j = t_j n_j$, $f_j = p_j t_j$, $g_j = r_I m_j$,

$m_j = 2 \ T_j \eta_{11} - S_j \eta_{10}$, $n_j = R \ S_j - i(E_a/q_\xi)(e_1 - e_3) \ s$,

$= (a, - a_3 \ S_j^2) \ c + 2 \ T_j S_j a_3 \ s$, 1 $L + K_2 S_j^1$,

$r_j = M + K_1 S_j^2 - (\epsilon_a/4\pi)(E_a/q_\xi)^2 \sigma_\perp (1+S_j^2)/\sigma_j - i(E_a/q_\xi) P S_j \sigma_a c /\sigma_j$,

$t_j = R \ S_j + i(E_a/q_\xi) \ \beta_j s$, $\sigma_j = \sigma_\perp(1 + S_j^2) + \sigma_a c$,

and $\beta_j = (e_1 - e_3) - P \ \sigma_a \ c / \sigma_j$.

Eqs.(7) and (13) together form a characteristic value problem and hence any arbitrary set of roots of Eq. (7) will not, in general, satisfy Eq.(13). In order to obtain the solutions we have to find a set of values of S_j that satisfy Eqs.(7) and (13) simultaneously.These calculations were done numerically. For a given set of values of the material parameters and a given value of a, we choose some values of the applied voltage V_a and δ and the roots of Eq.(7) are obtained. These are then substituted in Eq.(13) and the BVD is evaluated. The value of δ is then varied till the BVD becomes zero. The calculations are repeated for different values of the voltage. The lowest value of the voltage at which such solutions exist is the threshold voltage V_{th} . The above process is then repeated for different values of a. The lowest value of V_{th} gives the critical voltage V_c for the onset of the instability and the corresponding values of 6 and a give the magnitude and direction of the wavevector of the convective rolls, respectively.

4.3 RESULTS AND DISCUSSION

a. Calculations without flexoelectricity

In this case we get normal rolls at the threshold for the standard values of the MBBA parameters listed in table 1 of chapter 3. However, if the values of some of these parameters are suitably altered oblique rolls are obtained. For example, if the twist elastic constant K_2 is decreased slightly, with all other parameters having the standard MBBA values, a nonzero value of a can be obtained at the threshold. Similar results were obtained by Zimmermann and Kramer [3] using stress-free boundary conditions. In order to get a non-zero value of a at the threshold we have taken K_2 to be 2×10^{-7} dynes instead of the standard MBBA value of 4×10^{-7} dynes, with all other parameters as in table 1 of chapter 3. Fig.2 shows the variation of V_{th} with a obtained from the calculations.

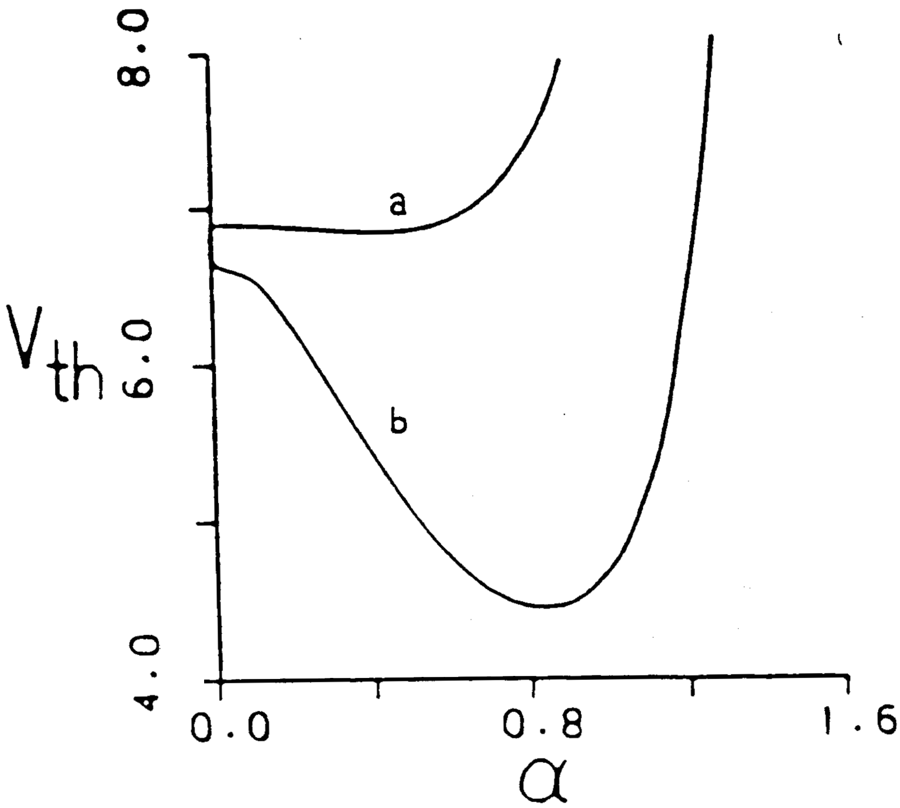

Fig.2. Variation of the threshold voltage (in Volts) with a (in radians). The curves labelled a and b correspond to calculations without and with flexoelectricity, respectively.

We have also calculated the variation of all the variables across the thickness of the sample at a voltage slightly above the threshold (Figs.3-7). As mentioned earlier, when the flexoelectric terms are neglected the roots of Eq.(7) occur in ± pairs. Therefore the profiles of all the variables are symmetric about the mid-plane of the sample. It should be noted here that the axial velocity v_η results from the oblique flow of the fluid in relation to , with a vertical velocity gradient. This situation is similar to the so-called nematic Hall effect [4], discussed in chapter 2. Fig.8 shows the trajectories of two fluid particles in adjacent rolls. The plane containing these trajectories is at an angle to the ξz plane because of the axial component of the velocity. The symmetry of the velocity profiles, however, results in closed trajectories of the fluid particles.

b. Calculations including flexoelectricity

In this case oblique rolls are obtained at the threshold for the standard MBBA values of the material parameters. However, for the sake of comparison with the previous case we retain the value of K_2 used in that section, ie, 2×10^{-7} dynes. The variation of V_{th} with a is shown in Fig.2. It is clear from the figure that flexoelectricity strongly favours oblique rolls. The difference in V_{th} at a = 0 between the two cases with and without flexoelectricity arises from the contribution of the flexoelectric polarization to the space charge density in the medium.

The variation of the different variables across the thickness of the sample calculated at a voltage slightly above the threshold voltage is shown in Figs.3-7. The odd powered terms in Eq. (7), which are present when the flexoelectric terms are taken into account, give rise to the asymmetry in their profiles. The strong coupling to the flexoelectric terms leads to a conspicous asymmetry in the Φ profile (Fig.5) and in turn to that in the v_η profile (Fig.7). The asymmetry in the v_η profile results in an open helical trajectory of the fluid particles within the convective rolls. Fig.9 shows the calculated trajectory of two fluid particles in adjacent rolls, close to the periphery of the rolls. It is clear that they spiral in opposite directions. It must however be noted that within the same roll the particles close to the axis of the roll spiral in one direction and those close to the periphery spiral in the opposite direction. This is clear from Fig.10, which shows the two halves of the v_η profile superposed. Further, as can be seen from the figure, the difference between the two halves of the v_η

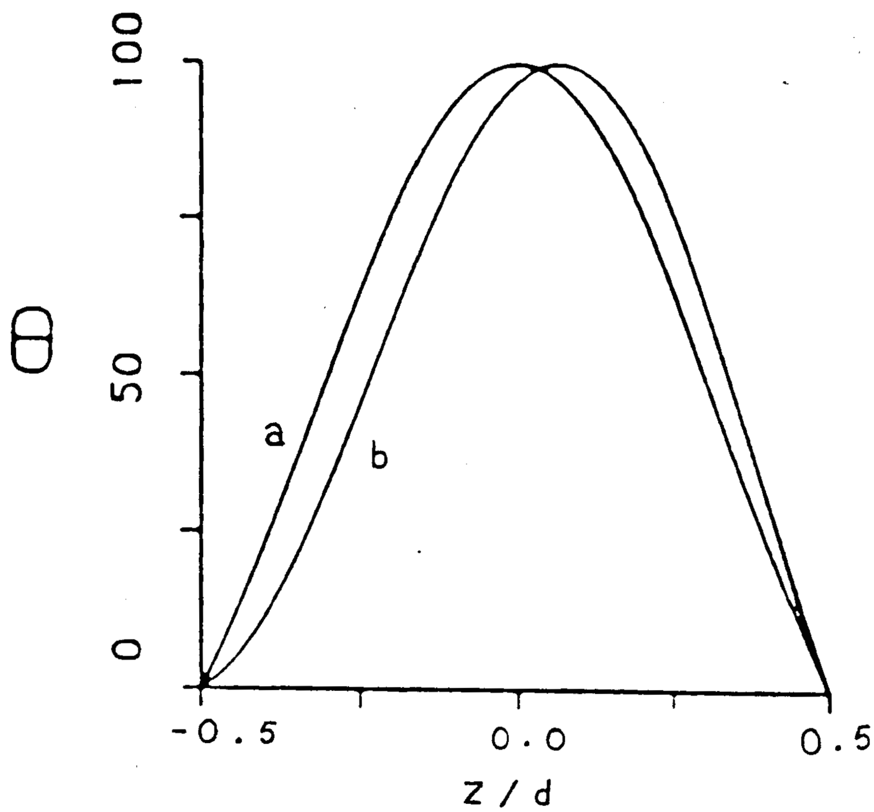

Fig.3. Variation of θ across the thickness of the cell at $\xi = 0$, ie, along the vertical line passing through the centre of the roll. The labels a and b have the same significance as in Fig.2.

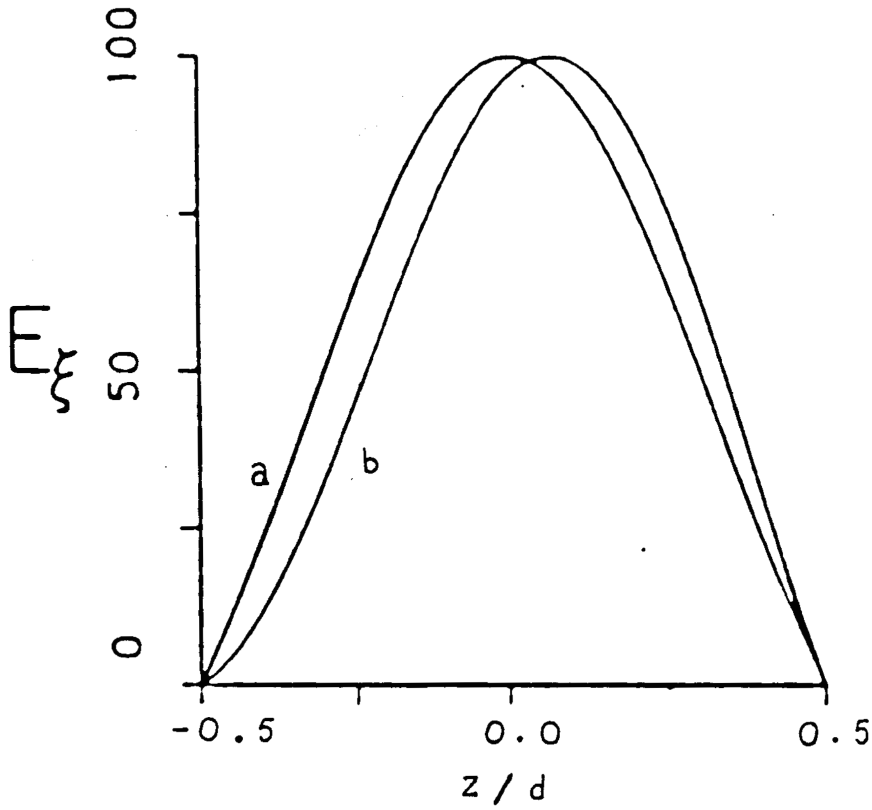

Fig.4. Variation of E_ξ across the thickness of the cell at $\xi = 0$. The labels a and b have the same significance as in Fig.2.

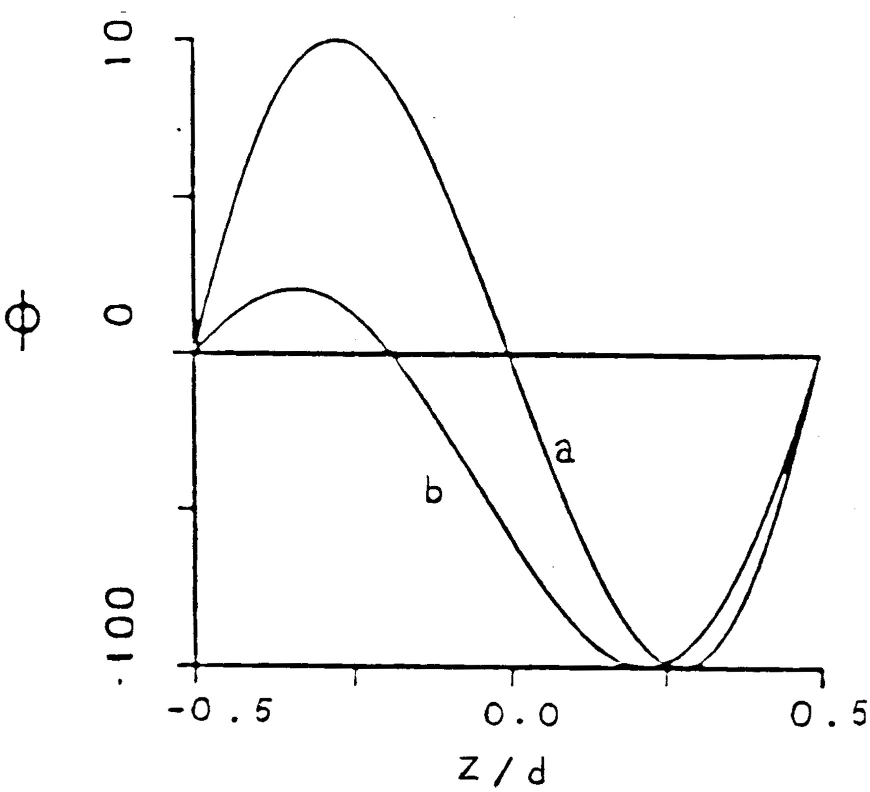

Fig.5. Variation of Φ across the thickness of the cell at $\xi = \pi/q_\xi$, ie, along a line passing through the edge of a roll. The labels a and b have the same significance as in Fig.2.

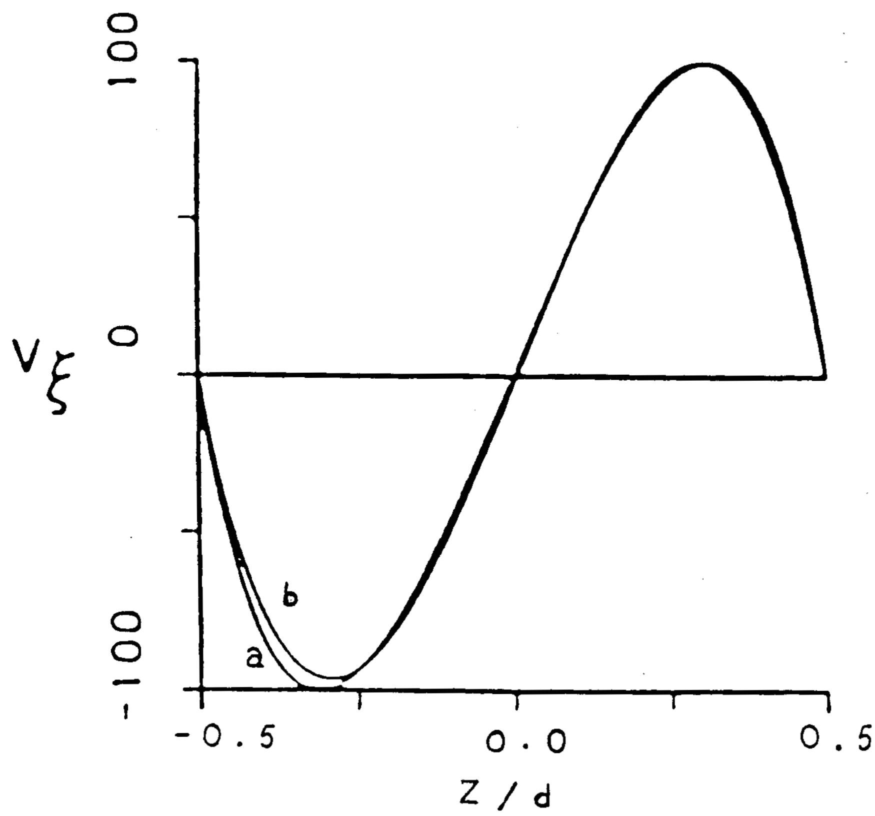

Fig.6. Variation of v_ξ across the thickness of the cell at $\xi =$ 0. The labels a and b have the same significance as in Fig.2.

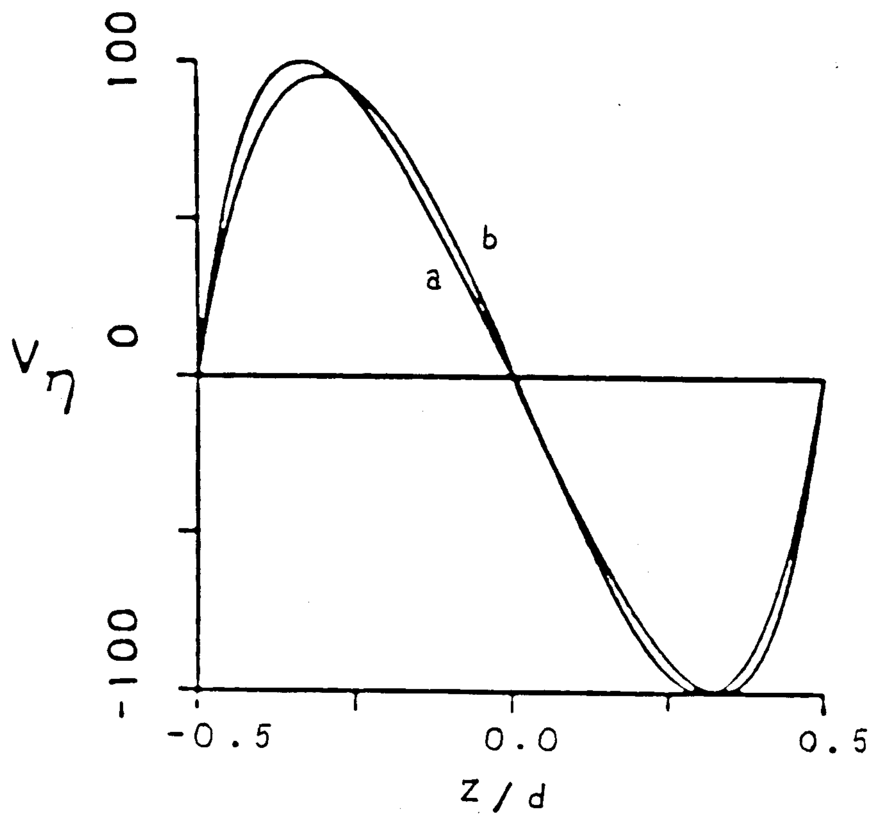

Fig.7. Variation of v_η across the thickness of the cell at $\xi = 0$. The labels a and b have the same significance as in Fig.2.

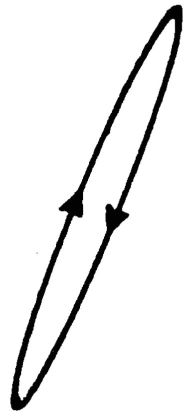

Fig.8. The closed trajectories of two fluid particles in adjacent rolls obtained from calculations without flexoelectricity. The ellipticity of the trajectories arises from a steep angle of viewing. Further, the scales along ξ , η and z have been chosen to be rather different for the sake of clarity.

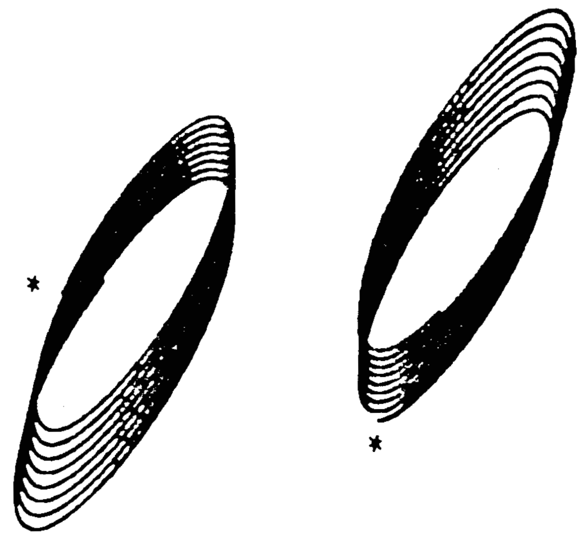

Fig.9. The helical trajectories of two fluid particles in neighbouring rolls obtained when the flexoelectric terms are included. The asterisks indicate the initial positions of the particles.

profile is relatively small close to the axis of the roll. Let us denote by $\bar{v}_\eta$ the net velocity along η of a fluid particle close to the periphery of the roll. From the above discussion it is clear that $\bar{v}_\eta$ is opposite in adjacent rolls with opposite vorticity. For a given sense of the vorticity $\bar{v}_\eta$ changes sign with either that of α or E_a, reflecting the flexoelectric origin of the helical flow.

4.4 EXPERIMENTAL STUDIES

In continuation of the studies on EHD instabilities under DC excitation, presented in the previous chapter, we have also made careful observations on the flow within the rolls. The trajectory of tracer particles could be clearly seen only when they were close to the periphery of the rolls. These particles were found to move along helical trajectories with particles in adjacent rolls spiralling in opposite directions. Further, the observed direction of $\bar{v}_\eta$ agrees with that obtained from the calculations for given signs of a, E_a and the vorticity. v_η was also found to change sign with that of any one of these three parameters, in agreement with the calculations.

Helical motion of the tracer particles within the convective rolls has been reported even under AC

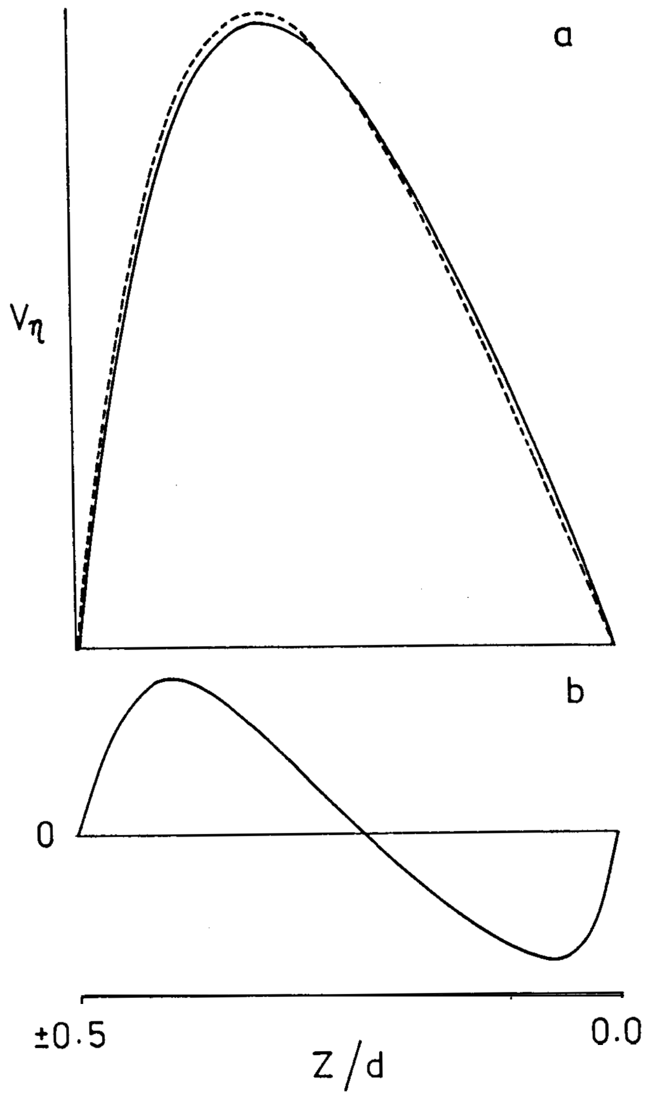

Fig.10. The two halves of the v_η profile shown superposed (a). The difference between the two halves is also shown on an expanded scale for clarity (b). It is clear from the figure that the net axial component of the velocity near the centre of the roll is relatively small and is in opposite direction to that near the periphery of the roll.

excitation [5,6]. But our calculations do not predict such a flow, as the direction of $\bar{v}_y$ is reversed when E_a changes sign. If the density of the tracer particles is very different from that of the nematic, then the trajectories of these particles will not be symmetric about the mid-plane of the sample. This can in principle give rise to a helical flow of the tracer particles, because of the Z dependence of the velocity profiles. It should be noted here that this effect will be present even if the velocity profiles are symmetric about the mid-plane of the sample and the motion of the fluid particles is confined to closed trajectories.

Recently Thom et al.[7] have also developed a three-dimensional analysis of the DC EHD instability in nematics taking into account the flexoelectric effect. In addition to a full numerical solution they also present solutions based on some trial functions. It is gratifying to note that their results are in agreement with those presented in this chapter.

Thus the three-dimensional analysis, which takes into account the rigid boundary conditions, confirm the importance of flexoelectricity in the oblique-roll instability in nematics under DC excitation. Further, it predicts a helical'flow of the fluid particles within the convective rolls. This prediction is confirmed by experimental observations.

REFERENCES

1. P.A. Penz and G.W. Ford, Phys. Rev., A6, 414 (1972).
2. S. Chandrasekhar, Hydrodynamic and Hydromagnetic stability, Oxford, Clarendon (1961).
3. W. Zimmermann and L. Kramer, Phys. Rev. Lett., 55, 403 (1985).
4. P. Pieranski and E. Guyon, Phys. Lett., A49, 237 (1974).
5. R. Ribotta, A. Joets and L. Lei, Phys. Rev. Lett., 56, 1595 (1986).
6. C. Hilsum and F.C. Saunders, Mol. Cryst. Liq. Cryst., 64, 25 (1980).
7. W. Thom, W. Zimmermann and L. Kramer, preprint (1988).